Journal of the Korean Electrochemical Society
Vol. 6, No. 3, 2003, 217-223

Characterization of Surface Roughness and Inhomogeneity of Hot-Rolled Carbon Steels by Using Image Analysis Method and Electrochemical Impedance Spectroscopy

Su-Il Pyun†, Kyung-Hwan Na, Joo-Young Go, and Jin-Ju Park

Department of Materials Science and Engineering, Korea Advanced Institute of Science and Technology, 373-1, Guseong-dong, Yuseong-gu, Daejeon, 305-701, Republic of Korea

(Received June 23, 2003 : Accepted August 11, 2003)

Abstract: The present work is concerned with characterization of surface roughness and inhomogeneity of four kinds of hot-rolled carbon steels in terms of the fractal dimension and the depression parameter by using image analysis method and electrochemical impedance spectroscopy, respectively. From the analysis of the 3D AFM image, it is realized that all the hot-rolled steel surfaces show the self-affine fractal property. The values of the fractal dimension of the hot-rolled steels were determined by the analyses of the AFM images on the basis of both the perimeter-area method and the triangulation method. In addition, the Nyquist plots were found to be depressed from a perfect semicircle form. From the experimental findings, the changes in the values of the fractal dimension and the depression parameter with chemical composition have been discussed in terms of the change in the value of hardness of base steel.

Key words : Fractal dimension, Depression parameter, Scaling property, Hardness of base steel

1. Introduction

Pickling is a chemical treatment used to remove the oxide scale from steel slabs by immersing in such hot acidic solutions as hydrochloric acid (HCl) and sulfuric acid (H_2SO_4)[1,2]. The oxide scale must be removed from hot-rolled carbon steels to prevent wear on dies and to avoid surface defects in the final product. After pickling, surface property of the hot-rolled carbon steels was conventionally examined by means of the naked eye, optical microscopy and whiteness measurement. However, these methods are much qualitative or uncertain ones for the examination of surface property.

Fractal geometry has been used to characterize disorderly structures in a wide range of different fields, and the use of fractal geometry to obtain a quantitative characterization of morphology of corroded surfaces has been described in several recent works[3-6]. Especially, considerable interest has been shown in the formation of rough surfaces[7,8].

In this respect, recently, many of our previous works[9-13] characterized surface property for transition metal oxide electrode[9], pitted electrode[10], platinum electrode[11] and carbon electrode[12,13] in terms of the fractal dimension.

The present work is aimed at characterizing such surface properties as surface roughness and inhomogeneity of the hot-rolled carbon steels in terms of the fractal dimension and the depression parameter, respectively. For this purpose, such image analysis methods as the perimeter-area and the triangulation ones were employed to determine the value of the fractal dimension of the surface of the hot-rolled steels. In addition, ac impedance measurements were carried out to measure the value of the depression parameter. The changes in the values of the fractal dimension, i.e., surface roughness, and the depression parameter, i.e., surface inhomogeneity, have been discussed in terms of the change in the value of hardness of base steel with respect to chemical composition.

2. Experimental

Four types of carbon steels for testing were produced at Pohang Iron & Steel Co., Ltd. (POSCO). The chemical compositions of the four carbon steels of 1, 2, 3 and 4 are shown in Table 1. All the steel specimens were hot-rolled at 860°-880°C and then pickled at 80°C in 10 wt.% HCl for 100s. As test solution, an aqueous 0.5 M Na_2SO_4 solution of 25°C was employed. A platinum gauze and a saturated calomel electrode (SCE) were used as the counter and reference electrodes, respectively.

Surface morphologies of the hot-rolled steels after pickling were obtained using atomic force microscope (AFM) (Digital Instruments Co. Dimension 3100). Scans were made on the specimens over areas from 45 μm × 45 μm with a resolution of 256 × 256 pixels. All AFM images were acquired at a probe scan rate of 1.0 Hz in an ambient air.

The topographic image data were converted into ASCII data which were then analyzed by the perimeter-area method and by the triangulation method to determine the self-affine

†E-mail: sipyun@webmail.kaist.ac.kr

Table 1. Chemical compositions of four kinds of the hot-rolled carbon steels (wt.%).

	C	Si	Mn	P	S	soluble Al	Fe
Specimen 1	0.034	0.002	0.18	0.012	0.012	0.040	Bal.
Specimen 2	0.002	0.002	0.21	0.015	0.012	0.032	Bal.
Specimen 3	0.155	0.014	0.66	0.011	0.007	0.028	Bal.
Specimen 4	0.0002	0.023	0.69	0.013	0.008	0.024	Bal.

and the self-similar fractal dimensions, respectively, of the hot-rolled steels. The software has been developed by Shin and Go[14] in our laboratory to determine the fractal dimension of the specimen from the analysis of the AFM image.

Ac impedance measurements were conducted using Zahner 6e impedance measurement unit. In order to determine the value of the depression parameter, impedance spectra were recorded on the hot-rolled carbon steels under open circuit conditions at room temperature in 0.5 M Na_2SO_4 solution. Impedance spectra were recorded from 10^5 Hz down to 10^{-1} Hz frequency using 5 mV amplitude perturbation. To evaluate the depression parameter, the measured impedance spectra were analyzed by using complex nonlinear least squares (CNLS) fitting method written first by Macdonald[15] and later modified in our laboratory[16].

3. Methods to Determine the Fractal Dimension of the Surface Using Atomic Force Microscopy (AFM)

There are two kinds of fractals in nature. One is a self-affine fractal which shows an anisotropic scaling behaviour. Here, the anisotropic scaling behaviour means that if a small piece of the fractal is blown up in an anisotropic way, i.e. a magnification by the factors depends on the direction, the enlarged version is made to match the whole object. The other is a self-similar fractal which shows an isotropic scaling behaviour. The self-similar fractal is magnified isotropically to observe the similarity at different scales.

Since the two kinds of fractals show the different scaling property, the fractal dimension of the fractal surface must be determined based on the inherent scaling property of the surface. In this section, two image analysis methods will be introduced to determine the fractal dimensions of both the self-affine and the self-similar fractal surfaces.

3.1. Perimeter-area method to characterize the self-affine fractal surface

The surfaces of the dense objects made by fracture, corrosion, deposition, etc. were usually believed to show a self-affine scaling property, i.e. an anisotropic scaling property perpendicular to the surface[17]. In order to characterize the self-affine fractal surface, the self-affine fractal dimension of the surface $D_{f,sa}$ has been determined by using the perimeter-area method[8,18-23].

Let us determine the self-affine fractal dimension of the hot-rolled steels, for example, used in this work. From the investigation of surface morphology using AFM, it is confirmed that the hot-rolled steels show an anisotropic scaling property perpendicular to the surface (see Section 4.1. for details). The algorithm used for determination of the self-affine fractal dimension by the perimeter-area method was as follows:

The scaling property of the hot-rolled steel surface is undoubtedly isotropic horizontally, i.e. the hot-rolled steel surface may be scaled with the same ratio in the x and y directions. Therefore, the intersection of the hot-rolled steel surface with a plane parallel to the (x,y) plane generates the self-similar lakes. It is well known[8,19] that the area A and the perimeter P of the self-similar lakes are related to their fractal dimension d_f by

$$P = \beta d_f A^{d_f/2} \tag{1}$$

where β is a proportionality constant. The self-affine fractal dimension of the cross-sectioned original surface $D_{f,sa}$ is related to d_f by

$$D_{f,sa} = d_f + 1 \tag{2}$$

The hot-rolled steel surfaces were cross-sectioned by a plane and then the perimeters and the areas of the resulting lakes were calculated. For instance, Figs. 1(a) and (b) depict the typical 3D AFM image of the hot-rolled carbon steel surface filled with water (black pixels) up to a height corresponding to 40% of the maximum height of the specimen surface and the corresponding 2D description of the perimeters (gray pixels) along with the areas (black pixels + gray pixels) of the self-similar lakes, respectively. Here, the gray pixels in Fig. 1(b) were defined as the black pixels neighbouring no black pixel. The perimeter and the area of each lake were estimated from the numbers of gray pixels and of [black pixels + gray pixels] for each lake, respectively.

This algorithm was programmed in Fortran 77 by Shin and Go[14] in our laboratory. After correcting the perimeter and the area of each self-similar lake, the perimeter was plotted as a function of the area on a logarithmic scale. From the linear relationship between the logarithmic perimeter and the logarithmic area, the self-similar dimension of the 2D lakes d_f was determined from Eq. (1) and then the self-affine fractal dimension of the 3D specimen surface $D_{f,sa}$ was determined from Eq. (2) as well.

3.2. Triangulation method to characterize the self-similar fractal surface

In order to characterize the 3D self-similar fractal surface, the self-similar fractal dimension of the surface $D_{f,ss}$ has been determined by using the triangulation method[8,17,24]. This method is exactly analogous to the Richardson method[7] for

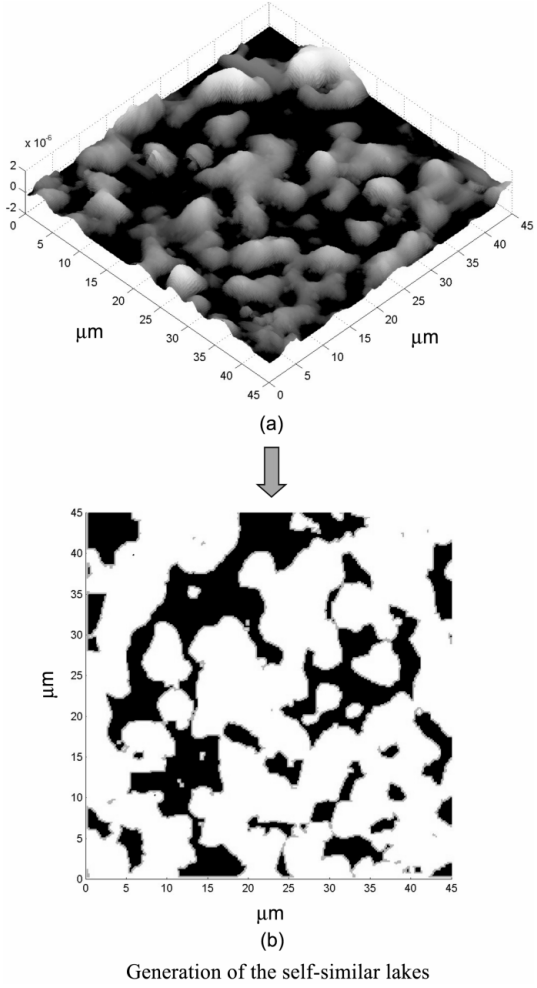

Fig. 1. (a) Typical AFM image of the hot-rolled carbon steel surface filled with water (black pixels) up to a height value corresponding to 40% of the maximum height value of the hot-rolled steel surface and (b) the corresponding 2D description of the perimeters (gray pixels) and areas (gray and black pixels) of the lakes.

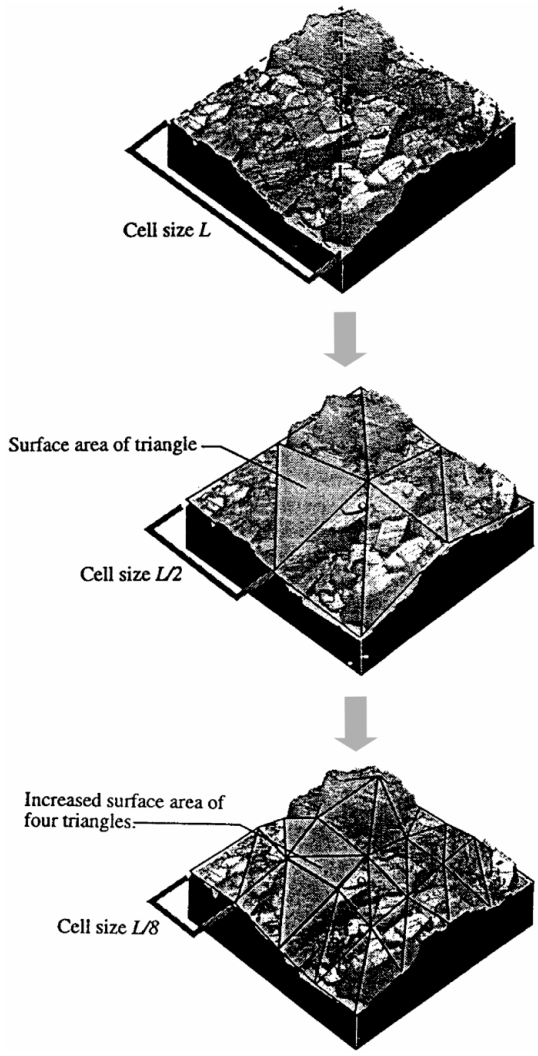

Fig. 2. Process of determination of the self-similar fractal dimension of the 3D surface by triangulation method.

a profile.

Fig. 2 describes schematically the algorithm used for determination of the self-similar fractal dimension of the self-similar surface by the triangulation method. The square (x,y) plane with a cell size L^2 is first divided into N^2 equal squares. This defines the location of the vertices of a number of triangles. Then the electrode surface is covered by $2N^2$ triangles inclined at various angles with respect to the (x,y) plane. These $2N^2$ triangles have the equal projected triangle size TS (= L/N), although their areas are different.

The scaled surface area SSA, i.e. the measured surface area by $2N^2$ triangles, is estimated to be the sum of the areas of all the $2N^2$ triangles. This measurement is iterated as decreasing projected triangle size TS, until every pixel in the AFM image serves as the vertices of the $2N^2$ triangles. Then, the 3D self-similar fractal dimension $D_{f,ss}$ of the surface is given by

$$D_{f,ss} = -\frac{d\log SSA}{d\log TS} + 2 \qquad (3)$$

This algorithm was also programmed in Fortran 77 by Shin and Go[14] in our laboratory. After correcting the scaled surface areas for the various projected triangle sizes, the scaled surface areas were plotted as a function of the projected triangle size on a logarithmic scale. From the linear relationship between the logarithmic scaled surface areas and the logarithmic projected triangle sizes, the self-similar fractal dimension of the surface was determined from Eq. (3).

4. Results and discussion

4.1. Surface morphologies of the hot-rolled carbon steels observed by AFM

Fig. 3 shows the AFM images of surface morphologies of four kinds of the hot-rolled carbon steels after pickling in 10 wt.% HCl solution at 80°C for 100s. The 3D AFM images exhibited the coarse protrusions with a lateral extent of 5-10 µm in the case of specimens 1 and 2, and the small protrusions with a lateral extent of 2-5 µm in the case of specimens 3 and 4. From the measured values of rms roughness of Table 2

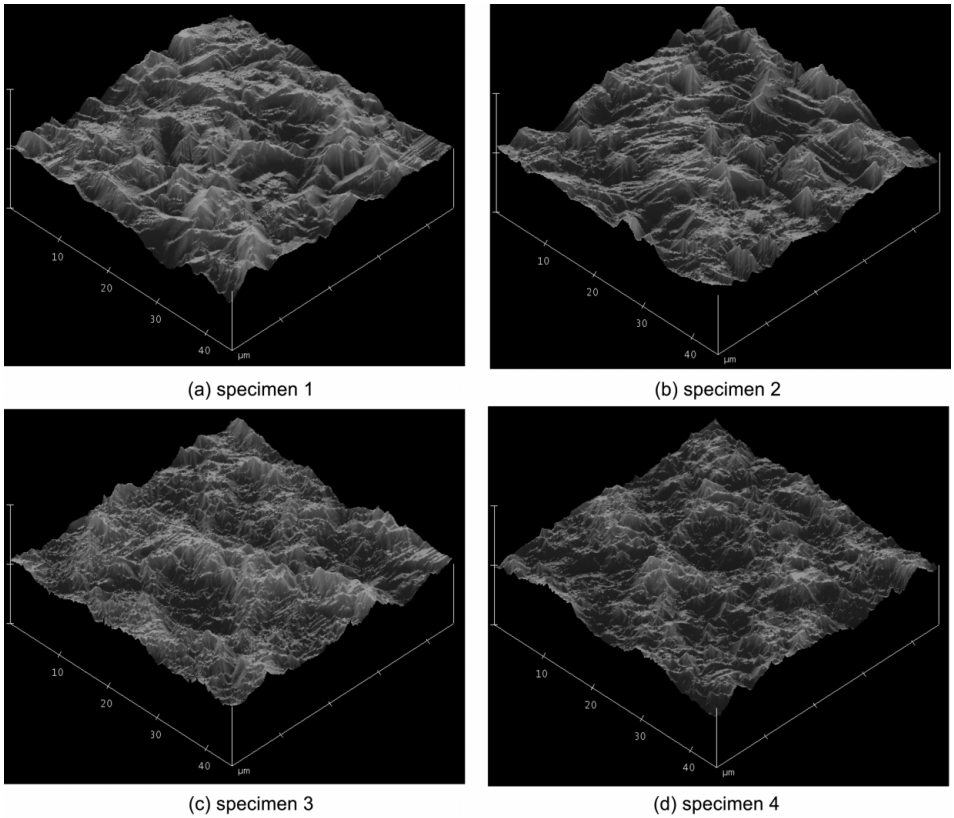

Fig. 3. 3D AFM images obtained from four kinds of the hot-rolled carbon steels after pickling in 10 wt.% HCl solution at 80°C for 100s.

(2nd column), it was observed that the value of rms roughness is much lower than that value of scale in the horizontal direction. From this, it is realized that the hot-rolled steel surface shows the self-affine fractal property.

4.2. The self-affine fractal dimension determined by the perimeter-area method and the self-similar fractal dimension by the triangulation method

Now, let us determine the self-affine fractal dimension of the hot-rolled steels. Fig. 4 illustrates typical logarithmic plot of the perimeter P and the area A for surface morphology of the specimen 1. The logarithmic P-A plot exhibited good linear relation above $A = 2\times 10^{-13}\ m^2$. However, it is worthy noting that another linear relation below $A = 2\times 10^{-13}\ m^2$ is physically meaningless due to the limitations of the AFM measurement[20]. The values of the fractal dimension of four kinds of the hot-rolled steels are listed in Table 2 (3rd column). It is seen that the value of the self-affine fractal dimension increased in sequence of specimens 1, 2, 3 and 4. Considering that the higher value of the fractal dimension represents the more roughened

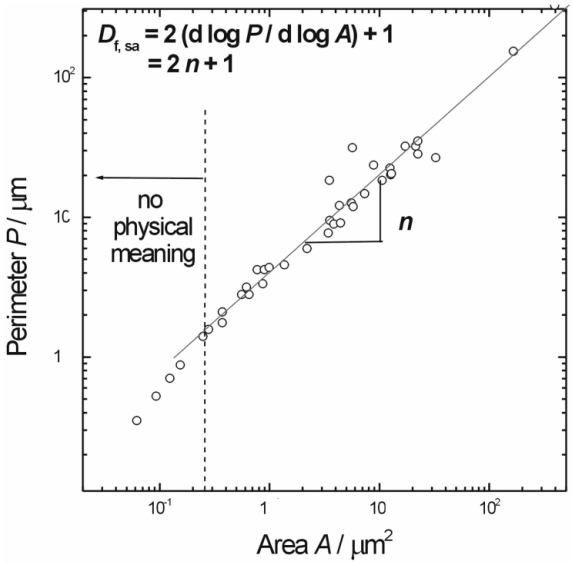

Fig. 4. Typical logarithmic plots of perimeter P and area A for surface morphology of the specimen 1.

Table 2. The values of RMS roughness and the fractal dimension for four kinds of the hot-rolled carbon steels.

Specimen	RMS roughness (nm)	Self-affine fractal dimension (by the perimeter-area method)	Self-similar fractal dimension (by the triangulation method)
1	491	2.324±0.048	2.036±0.001
2	507	2.432±0.060	2.038±0.002
3	548	2.436±0.028	2.051±0.002
4	457	2.494±0.034	2.051±0.002

surface, it is inferred that surface roughness increases in the order of specimens 1, 2, 3 and 4.

In our previous work[11], it should be emphasized that the self-similar fractal dimension described the anomalous current transient behaviour of the self-affine fractal electrodes in the case of the diffusion-limited current transient. Therefore, it is now necessary to determine the value of the self-similar fractal dimension although the hot-rolled steel surface shows the self-affine fractal property, in order to clarify the relationship between the self-affine fractal dimension and the self-similar one of the hot-rolled steels.

Fig. 5 gives the dependence of the scaled surface area SSA on the projected triangle size TS on a logarithmic scale obtained from surface morphology of the specimen 1. It was found clearly a linear relationship between log SSA and log TS, indicating the self-similar scaling property of the hot-rolled steel surface. The values of the self-similar fractal dimension estimated from Eq. (3) are listed in Table 2 (4th column). It is noted that the value of the self-similar fractal dimension increased in the order of specimens 1, 2, 3 and 4 in the same manner as the values of the self-affine fractal dimension determined by the perimeter-area method.

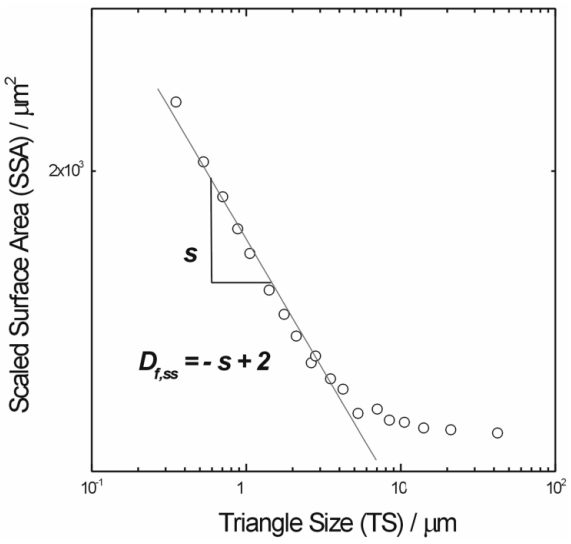

Fig. 5. The dependence of the scaled surface area SSA on the projected triangle size TS on a logarithmic scale obtained from surface morphology of the specimen 1. Here, s means *d*ln SSA/*d*ln TS.

Now, it is necessary to discuss the changes in the value of surface roughness with chemical composition. During the hot-rolling process, it is possible for the scale to stick in base steel. The scale stuck in base steel was experimentally undetectable by optical microscopy. Under the same rolling condition, hardness of base steel is closely related to surface roughness as follows: After pickling, most scale stuck in base steel were removed and thus groove was remained on base steel. Therefore, the number of remained groove on the specimen is under the control of the value of hardness of base steel. Consequently, remained groove leads to roughened surface. In other words, the higher number of remained groove implies the lower value of hardness of base steel. The schematic picture of the change in surface of the hot-rolled carbon steels with the value of hardness of base steel is given in Fig. 6.

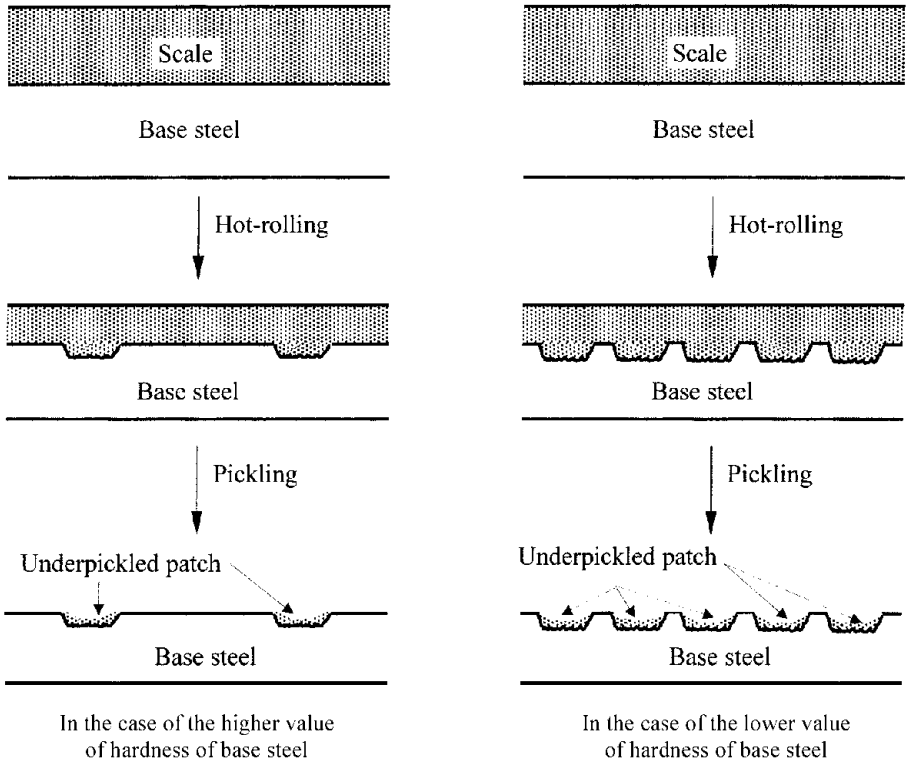

Fig. 6. Schematic picture of the change in surface of the hot-rolled carbon steels after hot-rolling and the subsequent pickling processes.

Table 3. Hardness of four kinds of the hot-rolled carbon steels in HRC. The result is the average of ten values.

Specimen	1	2	3	4
Hardness (HRC)	73	63	61	57

From the fact that surface roughness increased in the order of specimens 1, 2, 3 and 4, it is reasonable to say that the value of hardness of base steel decreased in that order. This is verified experimentally from the value of hardness of four kinds of the hot-rolled carbon steels as given in Table 3. The value of hardness of base steel is probably influenced by chemical composition of the specimen.

It should be stressed that there was a difference in the absolute value of the fractal dimension determined between by two image analysis methods. That is, the value of the self-affine fractal dimension determined by the perimeter-area method is always higher than that value of the self-similar fractal dimension determined by the triangulation method. This result is presumably due to the fact that the scaling property of the self-affine fractal surface in the vertical direction is different from that of the self-similar fractal surface. However, it is still unclear why the value of the self-affine fractal dimension is always higher than that of the self-similar fractal dimension. The above argument still needs further clarification.

4.3. Impedance behaviour of the hot-rolled carbon steels

In previous works from our laboratory[11,13], it was assumed that the ion movement towards the self-affine fractal electrode is isotropic in electrochemical system. Therefore, in this work, it is necessary to ascertain whether this assumption can be applicable to the hot-rolled steel surface or not.

Fig. 7 presents impedance spectra in Nyquist presentation obtained from the hot-rolled steels at open-circuit potential in 0.5 M Na_2SO_4 solution at room temperature. In this figure, it

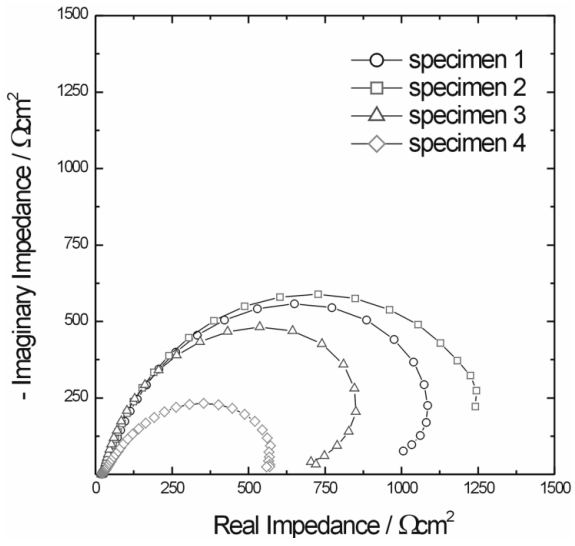

Fig. 7. Impedance spectra in Nyquist presentation obtained from the hot-rolled steels at open-circuit potential in 0.5M Na_2SO_4 solution at room temperature.

Table 4. Depression parameter determined from the impedance spectra in Nyquist plots for four kinds of the hot-rolled carbon steels.

Specimen	1	2	3	4
Depression Parameter	0.83	0.82	0.73	0.72

was found that all the Nyquist plots for the hot-rolled steels were found to be depressed from a perfect semicircle form. The occurrence of depression of impedance spectra can be described by the change in the value of the depression parameter. In order to determine the depression parameter, real and imaginary components of the measured impedance spectra were analyzed by using CNLS fitting method on the basis of a simple Randles circuit[15]. The resulting values of the depression parameter for four kinds of the hot-rolled steels are summarized in Table 4. It was observed that the value of the depression parameter decreased in sequence of specimens 1, 2, 3 and 4.

In recent years, it has been demonstrated by many researchers[25-27] that the deviation from a perfect semicircle form observed on a real electrode is intimately related to surface irregularity or surface inhomogeneity. For instance, for a perfectly smooth and homogeneous surface at all scales, the value of the depression parameter is unity. In contrast, if there are surface irregularity such as roughness or surface inhomogeneity such as underpickled patch, the value of the depression parameter is lower than unity. It was found from Table 4 that the values of the depression parameter for all kinds of the hot-rolled steels are lower than unity. Therefore, it can be deduced that lowered value of the depression parameter is due to observation of surface roughness or to existence of underpickled patch on the specimen.

In this respect, it should be discussed which factor between surface roughness and underpickled patch is predominant for the change in the value of the depression parameter. According to previous works[28-30], it is possible to convert the value of the depression parameter into that value of the fractal dimension when the occurrence of depression of impedance spectra is only caused by surface roughness. Therefore, in this case, it is necessary to determine the temporal cut-off ranges, i.e., inner and outer frequency cut-offs, in order to verify the dominant factor between surface roughness and existence of underpickled patch. It is generally agreed[30] that surface roughness l can be described in terms of frequency f, which is given by:

$$l = \frac{1}{2\pi\rho C_{dl} f} \tag{4}$$

where, ρ and C_{dl} mean the specific resistivity of solution and double layer capacitance, respectively.

By inserting the values of inner cut-off (2.5×10^{-7} m) determined by the perimeter-area method, ρ (0.0125 Ωcm) of test solution and C_{dl} (20 μF cm^{-2}), the value of frequency was calculated to be 2.5×10^{10} Hz. This means that it is possible to sense surface roughness in the frequency range of several tens of GHz. However, in the present work, the frequency ranges of impedance measurements are from 10^5 to 10^{-1} Hz.

From this, it is reasonable to say that the contribution of surface roughness to the change in the value of the depression parameter is negligibly small[13]. Consequently, existence of underpickled patch on the specimen mostly contributed to the occurrence of depression of impedance spectra. From the fact that the value of the depression parameter decreased in the order of specimens 1, 2, 3 and 4 from Table 4, it is concluded that the amount of underpickled patch increased in that order.

It should be emphasized that the amount of underpickled patch is closely related to the value of hardness of base steel like surface roughnes is associated with the value of hardness. In the case of the higher value of hardness of base steel, the number of remained grooves is relatively low after pickling. It is therefore expected that the amount of underpickled patch is also probably low. In contrast, in the case of the lower value of hardness, the amount of underpickled patch is high due to the higher number of remained grooves. The change in the amount of underpickled patch on the surface of the hot-rolled carbon steels with respect to the value of hardness of base steel is schematically shown in Fig. 6.

From the experimental findings, it is concluded that hardness of base steel contributes to both the changes of surface roughness and the amount of underpickled patch of the hot-rolled carbon steel in value. In addition, surface roughness and the amount of underpickled patch of the hot-rolled carbon steels can be quantitatively characterized by determination of the fractal dimension from image analysis method and the depression parameter from electrochemical impedance spectroscopy, respectively.

5. Conclusions

1. From the fact that the value of rms roughness is much lower than that value of scale in the horizontal direction by the observation of the 3D AFM images, it is suggested that the hot-rolled steel surface is characterized by the self-affine fractal property rather than the self-similar fractal property.

2. The values of the fractal dimension increased and at the same time those values of the depression parameter decreased in the order of specimens 1, 2, 3 and 4. This is attributable to the decrease in the value of hardness of base steel. Consequently, it is suggested that the value of hardness of base steel influences significantly both the variations of surface roughness and the amount of underpickled patch of the hot-rolled carbon steel.

3. Determination of the values of the fractal dimension and the depression parameter of the hot-rolled carbon steels proved to be more effective for characterizing surface roughness and the amount of underpickled patch, respectively, as compared with conventional observation by optical microscopy and whiteness measurement.

Acknowledgements

The receipt of a research grant for the 1-year period 2002/2003 from POSCO, Korea is gratefully acknowledged. Incidentally, this work was partly supported by the Brain Korea 21 project.

References

1. R. M. Hudson, D. W. Brown and C. J. Warning, *J. Met.*, **19**, 9 (1967).
2. R. M. Hudson, R. J. Joniec and S. R. Shatynski, “Pickling of Iron and Steel” in Metals Handbook, 9th ed., 68, Materials Park, OH: ASM International (1982).
3. G. S. Frankel, *Corros. Sci.*, **30**, 1203 (1990).
4. J. M. Costa, F. Sagues and M. Vilarrasa, *Corros. Sci.*, **32**, 665 (1991).
5. T. Holten, T. Jøssang, P. Meakin and J. Feder, *Phys. Rev. E*, **50**, 754 (1994).
6. L. Balazs and J. F. Gouyet, *Physica A*, **217**, 319 (1995).
7. B. B. Mandelbrot, “The Fractal Geometry of Nature”, 38, Freeman, Sanfrancisco (1982).
8. J. Feder, “Fractals”, Plenum, New York (1988).
9. H.-C. Shin, S.-I. Pyun and J.-Y. Go, *J. Electroanal. Chem.*, **531**, 101 (2002).
10. J.-J. Park and S.-I. Pyun, *Corros. Sci.*, **45**, 995 (2003).
11. J.-Y. Go, S.-I. Pyun and Y.-D. Hahn, *J. Electroanal. Chem.* **549**, 49 (2003).
12. S.-B. Lee and S.-I. Pyun, *J. Electroanal. Chem.* (2003) in press.
13. C.-H. Kim and S.-I. Pyun, *Electrochim. Acta* (2003) in press.
14. H.-C. Shin and J.-Y. Go, private communication, KAIST, Daejeon (2001).
15. M. C. H. McKubre, D. D. Macdonald and J. R. Macdonald, “Measuring Techniques and Data Analysis,” in Impedance Spectroscopy, ed. J. R. Macdonald, 179, John Wiley & Sons, New York (1972).
16. J.-S. Bae and S.-I. Pyun, *J. Mat. Sci. Letters*, **13**, 573 (1994).
17. J. C. Russ, “Fractal Surfaces”, Plenum Press, New York (1994).
18. B. B. Mandelbrot, D. E. Passoja and A. J. Paullay, *Nature*, **308**, 721 (1984).
19. B. B. Mandelbrot, *Physica Scripta*, **32**, 257 (1985).
20. J. M. Gómez-Rodriguez, A. M. Baró, L. Vázquex, R. C. Salvarezza, J. M. Vara and A. J. Ariva, *J. Phys. Chem.*, **96**, 347 (1992).
21. P. Herrasti, P. Ocón, R. C. Salvarezza, J. M. Vara, L. Vázquez and A. J. Arvia, *Electrochim. Acta*, **37**, 2209 (1992).
22. P. L. Antonucci, R. Barberi, A. S. Aricò, A. Amoddeo and V. Antonucci, *Mat. Sci. & Eng. B*, **38**, 9 (1996).
23. T. Silk, Q. Hong, J. Tamm and R. C. Compton, *Synth. Metals*, **93**, 65 (1998).
24. C. Douketis, Z. Wang, T. L. Haslett and M. Moskovits, *Phys. Rev. B*, **51**, 11022 (1995).
25. T. Pajkossy and L. Nyikos, *J. Electrochem. Soc.*, **133**, 2061 (1986).
26. T. C. Halsey, *Physical Review A*, **35**, 3512 (1987).
27. R. M. Hill and L. A. Dissado, *Solid State Ionics*, **26**, 295 (1988).
28. L. Nyikos and T. Pajkossy, *Electrochim. Acta*, **30**, 1533 (1985).
29. U. Rammelt and G. Reinhard, *Corros. Sci.*, **27**, 373 (1987).
30. T. Pajkossy, *J. Electroanal. Chem.*, **364**, 111 (1994).